Transition from extended-chain to once-folded behaviour in pure *n*-paraffins crystallized from the melt

John D. Hoffman*
Michigan Molecular Institute, 1910 W. St. Andrews Road, Midland, MI 48640, USA
(Received 6 July 1990; revised 6 September 1990; accepted 7 September 1990)

Nucleation theory is applied to extended-chain crystallization as background to the extended-chain to once-folded transition problem and certain unusual effects found in recent experiments. In the 'partial stem attachment' model employed, the activated complex leading to stem addition involves most of the length of the molecule, but only in the form of occasional contacts with the substrate. Here the lateral surface free energy σ is of mostly entropic origin. With a normal σ, the model gives the main features of the striking maximum in the extended-chain growth rate found by Ungar and Keller for n-$C_{246}H_{494}$. Complete register of the chain ends is not attained during nucleation, resulting in a transient layer of cilia on the crystal ('kinetic ciliation'). This layer leads to an end surface free energy σ', which is deduced from the growth rate data and used to estimate the initial thickness l_a of the unstable ciliated surface layer for *n*-$C_{246}H_{494}$. Shrinkage of l_a through annealing is discussed, with special reference to its effect on increasing the melting point toward its equilibrium value. This leads to an interpretation of the remarkable T' *versus* T_x plot for extended-chain *n*-$C_{192}H_{386}$ given by Stack and co-workers. Nucleation theory is employed to predict the temperature T_1^* at which once-folding begins in *n*-$C_{246}H_{494}$. With a normal value of the fold surface free energy (acting in a 'mean field' to account for chain end effects) the theory predicts both T_1^* and a marked increase in the growth rate of the once-folded species relative to that of the extended-chain at T_1^*. This explains the extended-chain to once-folded transition in *n*-$C_{246}H_{494}$, and also accounts for the previously unexplained minimum in the overall growth rate at T_1^* observed by Ungar and Keller. The treatment of the onset of once-folding is supported by data on other systems. The disordered nature of the initially-formed once-folded structure and its fate on annealing are discussed.

(Keywords: nucleation theory; crystallization; *n*-paraffin; extended-chain; once-folded chain; transition; surface free energy; surface disorder; kinetic ciliation; annealing; melting point)

INTRODUCTION

It is known that during isothermal crystallization from the melt, certain very long pure *n*-paraffins form only extended-chain crystals near the melting point, i.e. at a low undercooling, while at a lower temperature, T_1^*, once-folded species occur abruptly and in profusion. This effect occurs, for example, in the measurements of Ungar and Keller[1] for *n*-$C_{246}H_{494}$ and *n*-$C_{198}H_{398}$. These compounds are henceforth denoted C-246 and C-198, respectively, and similar notation will be employed for other *n*-paraffins later in this work. The transition from extended-chain to once-folded behaviour in these model compounds is of basic interest, since it relates to and illuminates the occurrence of chain folding in high polymers. From a thermodynamic standpoint, the extended-chain species is the most stable form, both at and below its melting point, so it is clear at the outset that the extended-chain to once-folded transition is beyond doubt a rate effect. Here we give a simple treatment of the transition in terms of nucleation theory.

Interest in the transition problem is heightened by the fact that in pure (monodisperse) C-246: (i) a maximum appears in the isothermal growth rate in the extended-chain domain and (ii) a minimum occurs in the growth rate at or near T_1^*, i.e. just at the onset of the once-folded domain. This situation is depicted in *Figure 1a*, which is based on the work of Ungar and Keller[1]. (The quantity $\tau_{0.1}$ is the time required to achieve 10% crystallization; here we employ the customary interpretation that $\tau_{0.1}^{-1}$ is at least approximately proportional to the lineal growth rate G.) Until now, the phenomena noted in (i) and (ii) above have been regarded as outside the reach of nucleation theory[1]. We shall show that both the maximum and minimum are natural consequences of an appropriate application of such theory. It is also noted that the same treatment that explains the maximum in the growth rate of extended-chain C-246 also explains the $G \propto \Delta T$ behaviour observed near the melting point in pure extended-chain C-94 as observed by optical microscopy[2].

Further details associated with extended-chain growth are considered. These include a discussion concerning: (1) the prediction that the extended-chain crystals of C-246 when first formed have a quite rough ciliated end surface of kinetic origin that is well in excess of the equilibrium roughness; (2) an estimate based on statistical mechanical considerations of the thickness l_a of the transient ciliated amorphous surface layer in the newly-formed region of an extended-chain crystal; (3) the annealing (thinning) of l_a on storage, including its effect on the melting point; and (4) the nature of the chain conformation in the activated state of the extended-chain nucleus as revealed by the apportionment factor ψ, and

* Present address: Department of Materials Science and Engineering, The Johns Hopkins University, Baltimore, MD 21218, USA

0032-3861/91/152828-14

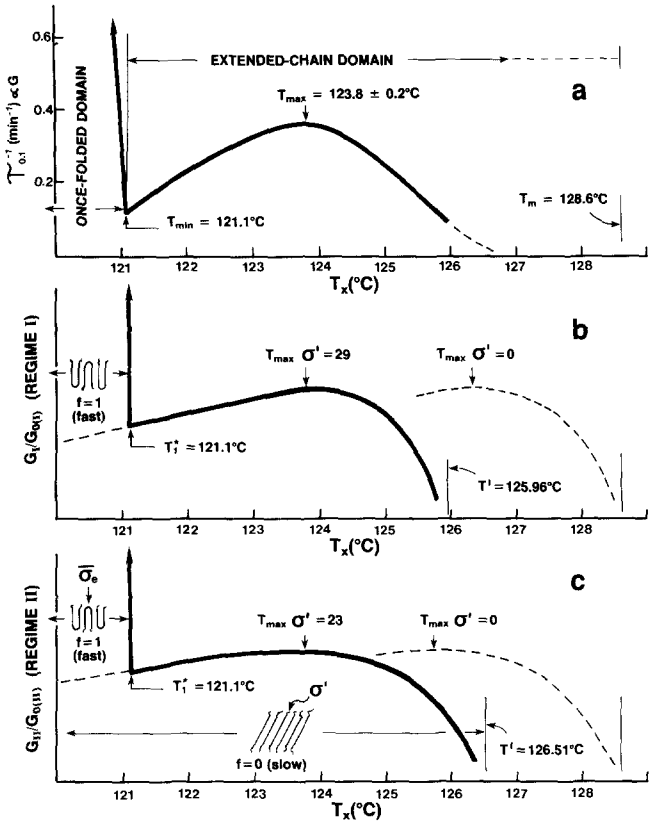

Figure 1 Growth rate of C-246 as function of isothermal crystallization near melting point showing extended-chain growth rate and onset of once-folding. (a) Data of Ungar and Keller[1] for C-246. (b) Theoretical curve for regime I. (c) Theoretical curve for regime II. Theoretical curves calculated with $\sigma = 13.8$ erg cm^{-2} and σ' values are shown. Position of T_{max} determines σ'; peak values of G at T_{max} scaled to same height

the relationship of this conformation to the origin of the lateral surface free energy σ.

The onset of once-folding, which begins at T_1^*, is discussed in terms of a nucleation-based theory developed earlier for poly(ethylene oxide) fractions[3]. For C-246, it is shown that a normal value of the fold surface free energy leads to a correct prediction of T_1^*, and that the rate of growth of the once-folded species will be much larger at and below T_1^* than that of the extended-chain type. The approach employed accommodates the significant finding of Ungar and Keller that the once-folded species begin their existence with a rather rough fold surface (so-called non-integral folding). The observation that these structures subsequently exhibit both thickening and thinning to more perfect extended-chain and once-folded crystals is discussed.

The present analysis centres mainly on melt-crystallized C-246 because of the wealth of experimental data available for it. However, the ability of the treatment to predict the onset temperatures in other systems is brought out in support of the overall approach.

ORIGIN OF THE MAXIMUM IN THE EXTENDED-CHAIN GROWTH RATE ABOVE T_1^*: ONSET OF ONCE-FOLDING AT T_1^*

Nucleation theory is first applied to extended-chain growth with the objective of showing that a maximum will appear in the growth rate somewhat below the melting point for n-paraffins similar in length to C-246. Then it is demonstrated, again with nucleation theory, that once-folded species will appear abruptly at a temperature T_1^* below this maximum. Finally, it is shown to be plausible that the once-folded structures will grow faster than the extended-chain type at and below T_1^*. This provides an explanation for the heretofore puzzling minimum in the overall growth rate at T_1^* in C-246 depicted in *Figure 1a*.

Extended chain growth rate

Consider first the isothermal formation from the melt of extended-chain species at low undercoolings. The main elements of the basic theory required have been given previously[2], though with a considerably different emphasis, and with some differences in detail. Therefore the treatment is outlined in the Appendix in compact form.

The barrier model employed to calculate the nucleation rate i and the substrate completion rate g is shown in *Figure 2a*. The forward and backward reaction rates A_0, B_0, A and B interact in such a way as to lead to the net flux S_T across the barrier which controls the overall surface nucleation rate and thence the rate at which a new layer of thickness b_0 is added[4]. This leads to the growth rate G. The addition of the first ($\nu = 1$) stem is by far the slowest process at normal undercoolings because it involves the lateral surface free energy σ, but the presence of the 'niche' on either side of the first stem eliminates this quantity from the energetics of the substrate completion steps ($\nu \geq 2$) which are more rapid and also lead the system into the stable region $\Delta\phi < 0$.

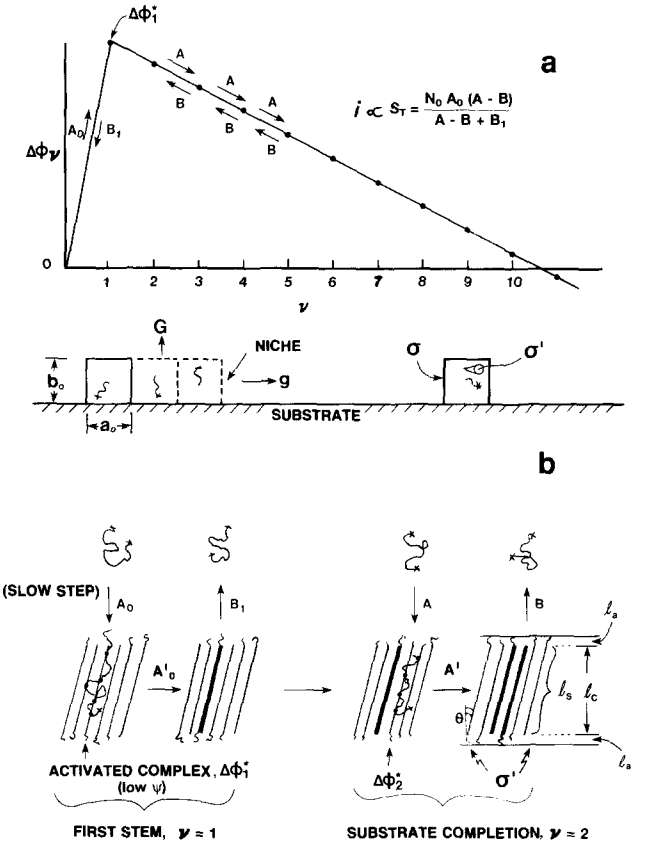

Figure 2 (a) Barrier system for surface nucleation and relation to surface energetics. (b) Molecular events involved in 'partial stem attachment' model for extended chains. Activated complex involves most of length l_0 of molecule

An additional purpose of the Appendix is to bring out the origin and role of the apportionment factor ψ, which can in principle vary between zero and unity. Within the constraints of the principle of detailed balance, the magnitude of ψ decides through the relation $\psi a_0 b_0 l_0(\Delta G)$ the fraction of the free energy of fusion per stem which has been attained as the activated state of stem addition is reached[4–6]. A low value of ψ, which is required by the data on C-246, has a definite physical meaning: it points directly to the fact that the activated complex in attachment of the first stem involves only occasional crystallographic or other attachments as depicted schematically in *Figure 2b*. (In the particular case of crystallization from solution, physical adsorption, in addition to crystallographic contacts, will play a role in restricting the configurations of a molecule on the crystal substrate. For the melt, the attachments are taken to be principally crystallographic in character.) A value of $\psi = 1$, which gives the full free energy of fusion per stem $a_0 b_0 l_0(\Delta G)$, holds only for over-simplified models, such as that which assumes instantaneous attachment of the whole stem as a unit, and does not correspond to experiment[4,5,7]. For low ψ, the bulk of the σ free energy is created during the 'partial stem attachment' stage comprising the activated complex, the fully aligned first stem forming shortly thereafter. Thus the lateral surface free energy σ is mainly a result of the considerable degree of immobilization of the molecule by the few attachments, and is therefore of mostly entropic origin. The partial stem attachment concept is not new and has been applied previously in the case of chain-folded systems[4,7]. It will be discussed further later in this work, with special reference to the extended chains. The analogue of *Figure 2b* relevant to chain-folded systems is depicted in Figure 27 of ref. 4.

A key point in the flux-based treatment of the nucleation and substrate completion process for extended chains is that in the rate-determining surface nucleus the effective (substantially immobilized) stem length is a constant equal (or closely so) to the chain length l_0, and is not to be treated as a variable as is appropriate in the case of chain-folded polymers where the stem length of the nucleus is l_g^*, which varies[4,8] as $C_1/(\Delta T) + C_2$. (Here ΔT is the undercooling and C_1 and C_2 are constants.) The 'or closely so' proviso above is inserted to cover the situation where the end surface is rough, i.e. has numerous emergent cilia, so that the actual nucleus length is slightly less than l_0. This leads directly to the additional key point that if the $-CH_3$ end surfaces of the nucleus and its substrate are rough, i.e. ciliated, one must introduce an end surface free energy σ' to account for it. Such roughness may be a result of a distribution of chain lengths (*structural ciliation*), which can lead to large initial values of σ' in the case of normal fractions with a distribution of molecular weight. Alternatively, we propose here the concept of *kinetic ciliation* wherein a σ' of moderate magnitude may arise in completely monodisperse materials of sufficient chain length because the chains forming the nucleus and its proximate substrate have not had sufficient time to complete the local rearrangements that permit the chain ends to achieve their minimal equilibrium roughness. We shall apply this concept in the following analysis of extended-chain growth in C-246.

The effective melting point depression caused by σ', whether it be of structural or kinetic origin, is given for an extended-chain system by:

$$T' = T_m[1 - 2\sigma'/(\Delta h_f) l_0] \quad (1)$$

where Δh_f is the heat of fusion, T_m the melting point of the pure compound that has attained its equilibrium degree of end-surface roughness, and l_0 the length of the molecule. The concept of a T' that is below T_m will affect the kinetics of extended-chain crystallization in our treatment of C-246. The equilibrium melting point T_m can be established with reasonable certainty by appropriate extrapolation procedures. (The rate effects attending the attainment of T_m will be discussed subsequently.) In what follows, the absolute undercooling is $\Delta T = T_m - T_x = T_m - T$ where T_x or T is the isothermal crystallization temperature. The value of T_m for C-246 is nominally 128.6°C (401.8 K). The relevant input data for C-246 are presented in *Table 1*.

According to the model described above and in the Appendix, the growth rate equation for extended-chain crystallization for a pure compound for regime I (single surface nucleus causes completion of substrate of length

Table 1 Input data for calculations on C-246

Quantity	Value	Source
a_0 = stem width	4.55×10^{-8} cm[a]	–
b_0 = layer thickness	4.15×10^{-8} cm	–
$a_0 b_0$ = cross-sectional area of chain	18.9×10^{-16} cm^2	–
l_0 = extended chain length	3.152×10^{-6} cm	Calc. as $246 \times 1.273 \times 10^{-8} + 2.0 \times 10^{-8}$ cm
Δh_f = heat of fusion	2.8×10^9 erg cm^{-3}[b]	–
Q_D^* = activation energy of diffusion in melt	5736 cal mol^{-1}[c]	Ref. 9
σ = lateral surface free energy	13.8 ± 2.1 erg cm^{-2}[d]	Ref. 2
T_m = extended-chain melting point	128.6°C[e]	Ref. 1
T_I^* = onset temperature for once-folding	121.1°C	Ref. 1
ΔT_I^* = undercooling at inception of once-folding	7.5°C[e]	Ref. 1
T_{max} = temperature at growth maximum for extended chains	123.8 ± 0.2°C	Ref. 1

[a] 10^{-8} cm = 1 Å = 0.1 nm
[b] 1 erg cm^{-3} = 10^{-7} J cm^{-3} = 10^{-1} J m^{-3}
[c] 1 cal = 4.184 J
[d] 1 erg cm^{-2} = 1 mJ m^{-2}
[e] Nominal value (see text)

$L = n_a a_0$) is:

$$G_I/G_{0(I)} = \exp -\frac{Q_D^*}{RT} \exp -\frac{2b_0\sigma l_0}{kT} \exp -\frac{2a_0b_0\sigma'}{kT} \times \left\{1 - \exp -\frac{a_0b_0}{kT}[l_0(\Delta G) - 2\sigma']\right\} \quad (2a)$$

extended-chain, regime I

Here the lineal growth rate is directly proportional to the surface nucleation rate i (see Appendix). An identical expression, except for a different G_0, holds for regime III. The corresponding expression for regime II (multiple nucleation on the substrate) has the growth rate proportional to $i^{1/2}$ and comes to:

$$G_{II}/G_{0(II)} = \exp -\frac{Q_D^*}{RT} \exp -\frac{b_0\sigma l_0}{kT} \exp -\frac{2a_0b_0\sigma'}{kT} \times \left\{1 - \exp -\frac{a_0b_0}{kT}[l_0(\Delta G) - 2\sigma']\right\} \quad (2b)$$

extended-chain, regime II

The quantity ΔG is the free energy of fusion per unit volume, which is given by:

$$\Delta G = \Delta h_f(\Delta T)/T_m \quad (2c)$$

where Δh_f is the heat of fusion.

The pre-exponential factors $G_{0(I)}$ and $G_{0(II)}$ in the case of general ψ each possess a factor $\exp[\psi a_0b_0l_0(\Delta G)/kT]$ as shown in the Appendix. For sufficiently small ψ, as for the nucleation model shown in *Figure 2b*, this factor remains near unity in the temperature range of interest here. The value of ψ is approximated by n^*/n where n^* is the number of crystallographic attachments per molecule in the activated complex, and n is the number of carbon atoms in the chain. If n^* is, say, 5–10, ψ is in the range 0.02–0.04 and there is little effect on the shape of the $G(T)$ curves. Substantially larger ψ lead to an increase in G with increasing undercooling sufficient to erase a maximum in the growth rate in the extended-chain domain.

In the above, G_I or G_{II} is the lineal growth rate (in centimetres per second, G_0 the preexponential factor (in the same units), Q_D^* the activation energy of transport in the melt, a_0 the molecular width, b_0 the layer thickness, a_0b_0 the cross-sectional area of the chain, and σ the lateral surface free energy. The factor in curly brackets { } in equations (2) describes the lessening activity of the backward reaction (stem removal) with increasing undercooling and leads to a $G \propto \Delta T$ growth law at very low undercoolings, which has been clearly observed[2] in pure zone-refined C-94. This effect arises directly from the factor $(A - B)$ in the expression for the total flux S_T (see Appendix and *Figure 2a*).

Figure 1b gives a plot of $G_I/G_{0(I)}$ as a function of T_x for C-246 in the extended-chain domain according to equation (2a) with σ set[2] at 13.8 erg cm^{-2} and T_m at 128.6°C for the cases $\sigma' = 0$ and $\sigma' = 29$ erg cm^{-2}. The other input data are given in *Table 1*. Similarly, *Figure 1c* gives $G_{II}/G_{0(II)}$ as calculated with equation (2b) for the cases $\sigma' = 0$ and $\sigma' = 23$ erg cm^{-2}. The σ' values in *Figures 1b* and *c* (bold lines) were chosen so that the calculated maximum coincided closely with the maximum in $\tau_{0.1}^{-1}$ found experimentally by Ungar and Keller[1] and depicted in *Figure 1a*. The initial upswing of G with decreasing temperature is a result of the lessening influence of the backward reaction, i.e. the term { } in equations (2); this term is the only one that involves the undercooling ΔT. At T_m (or T' if σ' is active) the forward and backward reactions are equal, and no net crystallization occurs. However, at the temperature of the maximum, T_{max}, the effect of the backward reaction and thus ΔT is mostly dissipated and the forward reaction governed largely by the factor $\exp(-2b_0\sigma l_0/kT)$ or $\exp(-b_0\sigma l_0/kT)$ becomes dominant. Recall that this factor reflects the work required for most of the length of the chain l_0 to form the σ surface free energy associated with what become the lateral surfaces of the nucleating stem. Together with the less important factors $\exp(-Q_D^*/RT)$ and $\exp(-2a_0b_0\sigma'/kT)$, if the latter is present, the treatment thus leads to the notable decrease in growth rate characteristic of essentially simple Arrhenius behaviour at temperatures below T_{max} whichever regime is assumed. Observe that the downturn in $G(T)$ below T_{max} is not a result of the intervention of a transport term of the form $\exp(-Q_D^*/RT)$ or $\exp[-U^*/R(T - T_\infty)]$ as is the case of chain-folded polymers at low temperatures[4]: the downturn in extended-chain C-246 below T_{max} is caused mainly by the fact that most of the length l_0 of the molecule participates in the activated complex as stated above.

It will emerge subsequently that the actual length of the chain involving σ in nucleus formation in C-246 is $l^* = l_0 - 2\bar{l}_{cil} \cong 0.84l_0$ where $\bar{l}_{cil}$ is the mean length of the cilia on either side of the crystal core of thickness l_c in the newly-formed region of the crystal (*Figure 2b*). On a more rigorous basis, the l_0 in equations (2) should be replaced by $l_0 - 2\bar{l}_{cil}$ so that the relevant energetic parameter governing the surface nucleation rate is $2b_0\sigma(l_0 - 2\bar{l}_{cil})$ rather than $2b_0\sigma l_0$. If this correction had been applied to the results for $G_I/G_{0(I)}$ and $G_{II}/G_{0(II)}$ shown in *Figure 1*, the differences would have been trivial.

The experimentally observed peak displayed in *Figure 1a* has been sketched from Figure 4 of ref. 1, which is for an unseeded specimen. Ungar and Keller refer to $\tau_{0.1}^{-1}$ in the aforementioned figure as the 'cleaner' parameter, and we have accordingly employed this plot for the purposes of comparing theory and experiment. In making this comparison, we have assumed that $\tau_{0.1}^{-1}$ is proportional to the lineal growth rate G. Exact conformance to this proportionality requires that the Avrami n_a be constant in the temperature range studied and that the crystals be born at the same time. The Avrami n_a is not precisely constant in the present case, but there is little doubt that a maximum actually occurs in $G(T)$ in the extended-chain domain. (The isotherms given by Ungar and Keller for 'unseeded' specimens in the extended-chain domain of C-246 correspond closely to an Avrami n_a of 3 at 122.3 and 123.3°C, while that for 124.8°C adheres to $n_a \cong 2.5$. The $n_a \cong 3$ isotherms likely correspond to spherulitic objects born at the same time. This is supported by data on pure C-94, which exhibits[2] spherulites born at or near $t = 0$ at low undercoolings. The $n_a \cong 2.5$ isotherm may represent the effect of an axialitic morphology, as found in polyethylene fractions at high growth temperatures[4]. A change of Avrami n_a with growth temperature will somewhat distort the shape of the growth curve if $\tau_{0.1}^{-1}$ is interpreted as being proportional to G, but will not cause a spurious maximum.)

While a seemingly better fit of the maximum might be obtained by adjustments of σ and σ', we set aside any such attempt until: (a) detailed $G(T)$ data are available by optical microscopy, these being free of disturbances resulting from changes in morphology and thence n_a; and (b) a more accurate T_m is obtained by the T' *versus* T_x method. As will be noted later, there is reason to believe that the true T_m estimated by the T' *versus* T_x method may be perhaps 1–1.5°C higher than 128.6°C. With such a T_m, σ' will be somewhat larger, but the minimum at T_1^* will remain. Even without such correction, the approximate correspondence of the overall features of the experimental and theoretical curves in *Figure 1* is sufficient to support the view that the basic physical cause of the maximum in the extended-chain growth rate of C-246 has been uncovered.

For low values of ψ corresponding to $n^*/n \leqslant 0.04$ for equation (2a) and $n^*/n \leqslant 0.02$ for equation (2b), the behaviour of $G_I/G_{0(I)}$ and $G_{II}/G_{0(II)}$ is essentially as depicted in *Figure 1*. (If the above values of ψ were tripled in each case, no maximum would be predicted.) Under the condition of low ψ the prediction of a growth rate maximum in the extended-chain domain in a pure *n*-paraffin with an l_0 close to that of C-246 is basically unavoidable. Values of σ in the range 13.8 ± 2.1 erg cm^{-2}, or even somewhat outside this range, still give the maximum, the larger values giving a somewhat sharper fall-off in G below T_{max}. Further, the presence of the maximum does not depend on whether or not σ' is invoked, though the position of the maximum does depend on this quantity (see *Figures 1b* and *c*). Neither is the particular value of the Avrami n_a critical to the prediction of a maximum, even in view of the possibility that the morphology, and hence the Avrami n_a, may change somewhat with crystallization temperature: the maximum occurs in G_I or G_{II} irrespective of the detailed connection these quantities may have with $\tau_{0,1}^{-1}$. Note also in *Figure 1* that the maximum appears no matter which regime is assumed, though it is somewhat more pronounced for regime I. In sum, the rate maximum in the extended-chain domain has a quite general and straightforward explanation in terms of nucleation theory as adapted to accommodate the partial stem attachment character of the activated complex in chain systems.

The successful prediction of the maximum in the extended-chain growth rate of C-246 is significant. First, it leaves little doubt that most of the molecule is involved in surface nucleus formation: the main nucleation barrier clearly involves l_0 except for that small portion involving the ciliation effect which is in any case separately accounted for by σ', as noted below. A more complete discussion of the circumstances attending the fact that most of the molecule of length l_0 contributes to the activated state is given later. As regards the generality of σ', it will develop later in this work that thermal and melting point data[10] for pure C-192 clearly imply that this parameter is also active in this material. The theory can accommodate regime transitions should they occur in the extended-chain region. (Consideration of equations (2a) and (2b) reveals that a change of slope in the growth rate *versus* T_x curve will occur in the vicinity of a I to II regime transition. However, as regime I behaviour gives way to regime II, the slope change can be positive rather than negative, which is the opposite of the usual case.) There is no clear intimation of a regime transition in C-246, but if one had occurred it would have merely distorted the shape of the maximum, rather than have caused it. A further justification for equations (2a) and (2b) is that they both lead to a $G \propto \Delta T$ growth law at low ΔT as has been fully verified[2] for C-94. Thus, the treatment given here has applications well beyond that of predicting a maximum.

A reasonable fit of the position of the rate maximum for regime I in the extended-chain domain of C-246 requires a value of the end surface free energy σ' in the vicinity of ~ 29 erg cm^{-2} (*Figure 1b*). This gives a T' in equation (1) of 125.96°C, corresponding to $\Delta T' = 2.64$°C. The corresponding results for regime II are $\sigma' \cong 23$ erg cm^{-2}, $\Delta T' = 2.09$°C, and $T' = 126.51$°C (*Figure 1c*). It is clearly evident that σ' participates in the surface nucleation process. The σ' values are rather insensitive to variations in the assumed value of σ. Considering the careful measures[11,12] taken to obtain pure C-246 for use in the experiments considered here, we favour the explanation that the excess end surface roughness leading to σ' in this case is that attributable to a completely monodisperse system, i.e. we take it to be an example of kinetic ciliation.

The concept of kinetically-induced surface roughness in chain systems was set forth many years ago in theoretical discussions for chain-folded crystals by Frank and Tosi[13] and by Lauritzen and Passaglia[14], the latter being the more general case because it allowed all possible fluctuations of stem length. Here the roughness refers to local fluctuations in the fold period, which become larger with increasing undercooling. Thus, from a theoretical point of view it is not only physically permissible but definitely to be expected that a kinetically-formed chain structure will initially exhibit some degree of surface disorder. (It is important to note further that Lauritzen and Passaglia showed that an equilibrium degree of fold surface roughness obtained at the melting point: we shall return to this point in connection with extended chains.) Subsequently, Ungar and Keller[1] suggested on the basis of their notable real-time SAXS results for C-246 that the transient precursor of the more regular once-folded structure exhibits what they termed 'non-integral' folding. The physical evidence for non-integral folding consisted of the fact that the structures originally formed exhibited a Bragg reflection somewhat greater than $l_0/2$ but much less than l_0. Our understanding of this effect is that the molecules are in fact almost entirely once-folded as suggested, the somewhat non-integral character of the folding being accounted for by the presence of surface roughness largely in the form of some ciliation together with a certain degree of looplike character in some of the folds (*Figure 3a*).

In view of the above theoretical calculations and experimental observations concerning chain-folded systems, our interpretation that some kinetic ciliation occurs at the early stages of formation of pure extended-chain crystals consisting of *n*-paraffin molecules of great length may be regarded as straightforward. At the same time, it is assumed that a small degree of roughness (equilibrium ciliation) will obtain at the true equilibrium melting point of an extended-chain system of high molecular weight. Subsequently, we shall describe the kinetic ciliation effect in extended-chain C-246 in some detail, but first it is convenient to consider the question of the onset of once-folding in C-246 in order to understand the origin of the minimum in the growth rate at T_1^*.

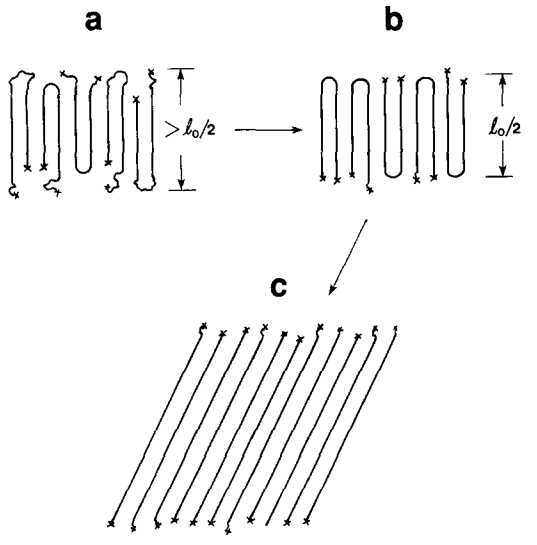

Figure 3 Once-folded species and annealing, schematic. (a) Initial once-folded structure with disordered surface ('non-integral folding'). (b) More perfect once-folded structure with large fraction of sharp folds. (c) Extended-chain structure, equilibrium state. Adapted from Ungar and Keller[1]. For discussion of slightly rough surface of equilibrium state of extended-chain structure, see text

The onset of once-folding in C-246

Consider now the undercooling ΔT_1^* where once-folding must begin in C-246. Elsewhere it has been shown on the basis of nucleation theory that for a sharp fraction whose molecules have a fixed mean length l_0 the undercooling ΔT_f^* at the onset of a domain with a specified number of folds per molecule is given for systems exhibiting 'quantized' chain folding by[3,15]:

$$\Delta T_f^* \cong \frac{2T_m\sigma_{e(\infty)}}{\Delta h_f}\left(\frac{f}{f+1}\right)\Big/\left[\left(\frac{l_0}{f+1}\right)-\delta\right] \qquad (3)$$

$$= 2T_m\sigma_{e(\infty)}f/(\Delta h_f)[l_0-(f+1)\delta]$$

where $f = 1, 2, 3, \ldots$ is the number of folds per molecule and $\sigma_{e(\infty)}$ is the surface free energy of a fold surface with no chain end effects as for $f \to \infty$. Here we extend the model originally proposed, which had closely matched chain ends at T_f^*, to allow some kinetic roughness in the form of loop-like character in some of the folds and a certain degree of ciliation of the chain ends at T_f^* (*Figures 3a* and *4a*). We subsume the energetic effects associated with ciliation at T_f^* in $\bar{\sigma}_e$ in the expectation that they are small compared to the contribution of the fold surface free energy. Further, it is recognized that $\sigma_{e(\infty)}$ may reflect the presence of some looplike folds, which may have a slightly different work of chain folding than the tight folds characteristic of the annealed once-folded state. The quantity δ, which is much smaller than $l_0/(f+1)$, is approximated as $kT/2b_0\sigma$. (The value of δ is close to $kT/b_0\sigma$ when the backward reactions are fully active, and close to $kT/2b_0\sigma$ when the backward reactions are relatively inactive (see ref. 7). At the undercooling ΔT_1^* in C-246, the backward reaction is nil, so $kT/2b_0\sigma$ is a reasonable approximation in the intended application.) Equation (3) is based in part on a simple mean field approximation where[3]:

$$\bar{\sigma}_{e(f)} = \sigma_{e(\infty)}\left(\frac{f}{f+1}\right) \qquad (4)$$

which accounts for dilution of the folds by chain ends or short cilia.

We now arrive at a point crucial to understanding the onset of f-folding. The derivation of equation (3) maintains that for chain-folded crystallization the stem length is a *variable* according to[3]:

$$l_g^* = \frac{2\bar{\sigma}_{e(f)}}{\Delta G} + \delta \qquad (5)$$

which is a formula of strictly kinetic origin of the form[3–5,8] $l_g^* = C_1/(\Delta T) + C_2$. (At T_f^* the fold period l_g^* is taken to be close to $l_0/(f+1)$.) Thus, a chain-folded system chooses its own nucleus stem length on a kinetic basis according to the undercooling involved irrespective of molecular length. It is essential to note this feature, which distinguishes it from the extended-chain case where the stem length of the nucleus is a constant close to l_0. As will be demonstrated shortly, this distinction leads to quite different kinetics in the two cases. The decrease of l_g^* with increasing undercooling is the basic cause for a molecule of fixed length l_0 exhibiting more folds per molecule with decreasing crystallization temperature, as illustrated schematically in *Figure 4a*. Equation (3) applies just at T_f^* where the ciliation, though present, is minimal (large dots on l_g^* curve in *Figure 4a*). At lower

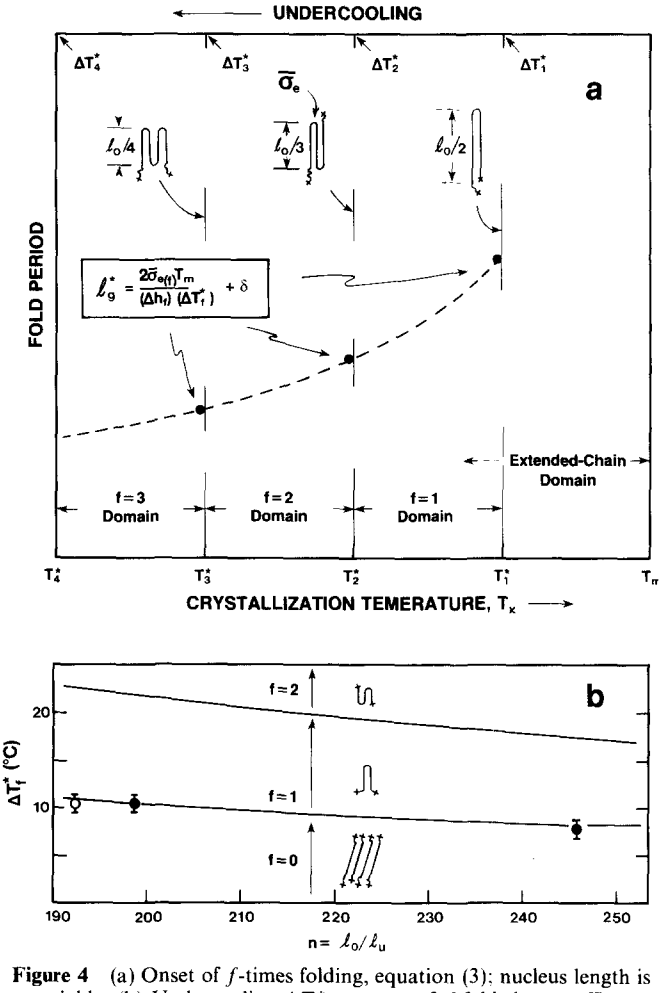

Figure 4 (a) Onset of f-times folding, equation (3); nucleus length is a variable. (b) Undercooling ΔT_f^* at onset of f-folded n-paraffins as function of chain length. Solid lines by equation (3) with $\sigma_{e(\infty)} = 90$ erg cm^{-2} and $\sigma = 13.8$ erg cm^{-2}. Solid circles on $f = 1$ line are for C-198 and C-246, Ungar and Keller[1]. Open circle on $f = 1$ line is for C-192, Stack *et al.*[10] (see text)

growth temperatures within a specified quantized fold domain, the diminishing value of l_g^* leads to increased ciliation in the initially-formed structures which tend to thicken first[3] to $l_0/(f+1)$ and later even further. The quantity l_g^* has no meaning at growth temperatures significantly above T_1^*, and extended-chain crystallization is therefore dominant in this $f=0$ domain as discussed previously.

Equation (3) successfully treats in quantitative detail[3] the onset temperatures of poly(ethylene oxide) fractions crystallized from the melt that exhibit quantized once-, twice-, three- and four-times chain folding (i.e. $f=1$–4) for specimens with fixed l_0 values ranging from 12 nm to 63.2 nm (data of Kovacs and co-workers[16–20]). This shows that the onset of quantized folding is a matter of both the undercooling and the overall chain length, and that the mean field approximation for $\bar{\sigma}_e$ is closely valid in this case. Therefore the problem of the onset undercooling ΔT_1^* for the once-folded domain ($f=1$) for C-246 may be approached with some confidence. Despite the somewhat disordered nature of the initially-formed surface, it can be safely assumed that each molecule has one fold and that the mean field approximation for $\bar{\sigma}_e$ is reasonable in this application.

Using equation (3) for C-246 with $f=1$, $\sigma_{e(\infty)}=80$ erg cm^{-2}, Δh_f from *Table 1*, and $T_m=128.6$°C it is found that $\Delta T_1^*=7.5$°C, corresponding to $T_1^*\cong 121.1$°C. Within experimental error, this is the temperature at which once-folded species first appear in profusion (*Figure 1*). This value of $\sigma_{e(\infty)}$ is within the acceptable range for a linear hydrocarbon chain, though it is somewhat smaller than the ~90 erg cm^{-2} often quoted in connection with kinetic studies on polyethylene[4,6,7,15]. If the true equilibrium T_m of C-246 is slightly higher than 128.6°C as proposed earlier, $\sigma_{e(\infty)}$ would be larger than 80 erg cm^{-2}. (An assumed T_m of 129.6°C gives a $\sigma_{e(\infty)}$ of 90.6 erg cm^{-2}, and a T_m of 130.1°C gives 96 erg cm^{-2}.) In any case it is evident that the mean field approximation expressed by equation (4) is valid within rather narrow limits for C-246. Further, it is clear that equation (3) is applicable even though the initially-formed once-folded species at T_1^* exhibits a rough surface. On no account is the abrupt appearance of the once-folded species at $T_1^*\cong 121.1$°C surprising.

Figure 4b shows the estimated onset undercoolings for *n*-paraffins of various different fixed lengths as calculated with equation (3) with $\sigma_{e(\infty)}=90$ erg cm^{-2} and $\sigma=13.8$ erg cm^{-2} (solid lines). The data points (solid circles) shown on the once-folded ($f=1$) line are those of Ungar and Keller[1] for C-198 ($\Delta T_1^*\cong 10\pm 1$°C) and C-246 ($\Delta T_1^*\cong 7.5$°C). Also shown is a data point for C-192 based on the work of Stack *et al.*[10]. (Calculations for C-192 with equation (3) with $\sigma_{e(\infty)}=90$ erg cm^{-2} and the true T_m of 127.5°C obtained from a T' *versus* T_x plot[10] give $\Delta T_1^*\cong 10.9$°C, corresponding to $T_1^*\cong 116.6$°C. The $\tau_{0.05}^{-1}$ data of Stack *et al.*[10] show a marked positive change of slope at $T=117\pm 1$°C ($\Delta T=10.5\pm 1$°C). These authors attribute one of the double melting point effects at 116°C to a 'non-integral non-extended' form; this effect is absent at 117°C, and we interpret this to mean that once-folding of the type illustrated in *Figure 3a* begins between 116 and 117°C. The experimental value of $\Delta T_1^*=10.5\pm 1$°C for C-192 is shown in *Figure 4b* as an open circle. Considering the indicated presence of a non-integral non-extended form, the upturn in $\tau_{0.05}^{-1}$ at ~117°C in Figure 10 of ref. 10 is most likely connected with the onset of once-folding rather than the result of a regime transition.) The data points for C-192 and C-198 would appear to be predicted quite well with a $\sigma_{e(\infty)}$ of 85–90 erg cm^{-2}, which is well within the acceptable range. The data point for C-246 is ~1°C low when compared with ΔT_1^* calculated with a $\sigma_{e(\infty)}$ of 90 erg cm^{-2}, but as explained earlier this may well be a result of T_m also being too low. The above ΔT_1^* values are in fair accord with earlier predictions[15]. There are no experimental results for isothermal crystallization from the melt showing twice- or three-times folding for *n*-paraffins in this l_0 range, doubtless because of experimental difficulties arising from the rapidity of the crystallization. The picture is much more complete for poly(ethylene oxide) fractions, which is attributable to the more convenient kinetics encountered in the chain length range studied.

Several more points are worth consideration prior to discussing the minimum in the growth rate at T_1^*. First, it cannot be emphasized too strongly that the onset of chain folding is not associated solely with the attainment of some unique chain length independent of other considerations, but is instead a function of both the undercooling and the chain length as equation (3) shows. In accord with this expression, very large undercoolings attainable only by strong quenching were required to induce once-folding in short *n*-paraffins such as a C-123 fraction[21,22], whereas once-folding was readily found at low undercoolings in C-246. That large undercoolings are required to induce once-folding as shorter chains are considered is particularly clear in the case of poly(ethylene oxide) fractions[3].

The second point deals with the fate of once-folded structures formed from the melt that initially have rough surfaces. As noted by Ungar and Keller and co-workers[1,23] the rough surface becomes more even on initial storage, producing rather perfect crystals with a thickness that is very close to $l_0/2$ and which exhibit better folding (*Figure 3b*). (Once-folded crystals of C-198 grown from dilute solution exhibit excellent perfection indicative of very little surface disorder and a high degree of adjacent re-entry[24].) This process involves a thinning[1] of the original structure because of the removal of cilia and looplike folds through chain translation. The thinning effect (which will be seen later to have its counterpart for extended-chain structures) is clearly driven by the free energy reduction associated with the removal of the emergent cilia and chain-end defects in the crystal, and possibly by the conversion of looplike folds to lower energy tight folds. The adjacent re-entry in these rather perfect annealed once-folded structures (*Figure 3b*) was likely present to a considerable degree in the kinetically-determined original structures because of the niche effect. Even so, these once-folded crystals themselves subsequently undergo thickening at various rates depending on storage time and temperature, thereby approaching the equilibrium extended-chain state as depicted in *Figure 3c*. Thus it is that just below T_1^* thickening and thinning were observed simultaneously in C-246.

Finally, it is worth noting the parallel between the energetic quantities found here for C-246 and related *n*-paraffins and those obtained from chain-folded polyethylene fractions. Based on the previous discussion, the best value of $\sigma_{e(\infty)}$ from ΔT_1^* is around 85–90 erg cm^{-2}. A value of $\sigma_e=93\pm 8$ erg cm^{-2} is found for

polymeric specimens by the T' *versus* $1/l$ thermodynamic method[4], and the value 90 erg cm^{-2} finds satisfactory application[7] in polyethylene fractions of $M_w \approx 1.8 \times 10^4$ to 1.2×10^5. Thus the fold surface free energy appears to hold over a wide range of molecular weights, even though estimated by very different routes. The value $\sigma = 13.8 \pm 2.1$ erg cm^{-2} covers all previously known estimates for *n*-paraffins C-15 and higher as well as polyethylene fractions[2]. The σ for *n*-paraffins may be subject to emendation depending on the best value required to explain in detail the maximum in the extended-chain growth rate of C-246 when accurate T_m and $G(T)$ data become available.

Estimated relative rates of growth of extended-chain and once-folded crystals: the minimum in overall growth rate near T_1^* *in C-246*

Consider now the question of the cause of the minimum in the overall growth rate. Observe in *Figure 1* that the onset of once-folded crystallization at $T_x \cong 121.1$°C for C-246 corresponds to the position of the minimum in the growth rate, i.e. $T_1^* = T_{min}$. The maximum in the extended-chain growth rate has already been explained. Then to predict this minimum requires that a rationale be given for the once-folded species having a considerably higher growth rate than the extended-chain form just at and slightly below $T_1^* \cong 121.1$°C. This rationale is given below. The treatment is in a number of respects highly approximate, but still sufficient to justify a considerable difference in rate. In the following the growth rate of the extended-chain species at T_1^* is denoted $G_{(f=0)}$ and the corresponding growth rate for once-folded structures $G_{(f=1)}$. While it is certain from the work of Ungar and Keller[1] that the ratio $G_{(f=1)}/G_{(f=0)}$ at T_1^* is very large, perhaps 100 or more, there is currently no quantitative information on its exact value. Accordingly the discussion below is restricted for the most part to general considerations. For reasons of simplicity, it is assumed that both the extended-chain and once-folded species crystallize in regime II at T_1^*. A parallel argument holds if both forms crystallize in regime I, or if the extended form is in regime I and the once-folded form in regime II.

There is a simple way to see from a general perspective why the once-folded species grow more rapidly than the extended-chain type at T_1^*. Recalling that $l_g^* = 2\bar{\sigma}_{e(f)}T_m/(\Delta h_f)(\Delta T) + \delta$, and for the time being neglecting δ, and noting for $f = 1$ that $l_g^* = l_0/2$, one finds for the once-folded case at T_1^*:

$$G_{II(f=1)} \propto \exp -\frac{2b_0\sigma\bar{\sigma}_e T_m}{(\Delta h_f)(\Delta T_1)kT_1^*} \cong \exp -\frac{b_0\sigma l_g^*}{kT_1^*}$$

$$= \exp -\frac{b_0\sigma(l_0/2)}{kT_1^*} \qquad (6a)$$

This is a straightforward adaptation of current nucleation theory for chain-folded systems for regime II, wherein σ_e is replaced by $\bar{\sigma}_e = \sigma_{e(\infty)}[f/(f+1)]$ and T by T_1^* (see equation (A-11) in Appendix). From equation (2b) the corresponding expression for extended chains is:

$$G_{II(f=0)} \propto \exp -\frac{b_0\sigma l_0}{kT_1^*} \qquad (6b)$$

The factor enclosed by { } in equation (2b) is essentially unity at T_1^*, and is therefore omitted, as is the unimportant factor $\exp(-2a_0b_0\sigma'/kT)$. Thus the stem length controlling the nucleation act is close to $l_0/2$ for the once-folded case and close to l_0 for extended chains. This difference in effective stem length highlights the main reason that once-folded systems will grow considerably faster at and below T_1^* than will those crystallizing in the extended-chain mode for pure materials with chain lengths similar to C-246. With the maximum in the growth rate above T_1^* having been justified previously, and with the foregoing rationale rendering plausible very rapid growth of once-folded species beginning at T_1^*, the presence of a minimum in the overall growth rate, as depicted in *Figure 1a*, is seen to be a natural consequence of the relevant expressions of nucleation theory. (By a consideration of fluctuations in l_g^*, the simple treatment given here can be modified to give a steep rise with finite slope beginning at T_1^* in the once-folded growth rate of the type shown in *Figure 1a* instead of a discontinuous increase.)

It is possible to make further progress with the help of equations (6), specifically with respect to what obtains for somewhat different l_0. The ratio $G_{II(f=1)}/G_{II(f=0)}$ may be written, to a sufficient approximation for present purposes, as:

$$\frac{G_{II(f=1)}}{G_{II(f=0)}} \simeq K \exp \frac{b_0\sigma(l_0/2)}{kT_1^*} \qquad (7)$$

Trends can be discerned by assigning a fixed value to K. Assuming the above ratio is 50 at T_1^* for C-246, one finds with $\sigma = 13.8$ erg cm^{-2}, $l_0 = 3.152 \times 10^{-6}$ cm, and $T_1^* = 121.1$°C that $K \sim 3 \times 10^{-6}$. If equation (7) is now applied to, say, C-190, for which $l_0 = 2.439 \times 10^{-6}$ cm and T_1^* is estimated on the basis of $T_m \cong 127$°C and equation (3) with a $\sigma_{e(\infty)}$ of 80–90 erg cm^{-2}, the ratio $G_{II(f=1)}/G_{II(f=0)}$ is found to be of the order of unity. From this point of view the abrupt rise at T_1^* seen in C-246 resulting from the onset of once-folding would not be expected for significantly shorter chains. Rather than considerably different growth rates, there should simply be a change of slope in the growth rate curves as once-folding begins. Examples of this type are known for poly(ethylene oxide) fractions[16,17].

In summary, the difference in stem lengths of the general type noted in equations (6) may reasonably be taken as the root cause of the greatly different rates of growth of the once-folded and extended-chain species for C-246 apparent near T_{min} in *Figure 1a*. Calculations suggest that such a marked difference may not appear for significantly shorter *n*-paraffins.

A final point deserves mention. Note that for C-246 the rate of formation of extended-chain crystals is predicted to remain finite below T_1^* even though the growth rate of the once-folded species is considerably faster there (*Figures 1b* and *c*). Thus, below T_1^* the once-folded and extended-chain crystal types are to some extent in competition in the kinetic sense, though the once-folded species is clearly predominant in this chain length range.

EXTENDED-CHAINS: NATURE OF AMORPHOUS SURFACE LAYER, ANNEALING, AND MOLECULAR CONFIGURATIONS IN THE NUCLEUS

It is possible to draw a number of inferences from the fact that a relatively large σ' is required for C-246 to account for the observed position of T_{max} in the extended-chain domain (*Figure 1*). In particular, it will

be shown that the 'rough' or disordered surface implied by the σ' associated with the initially-formed transient extended-chain structure is reasonably described as consisting of an amorphous layer of cilia of varying lengths. An approximate estimate is given of the initial thickness of this layer and of its eventual fate through annealing. Further, from a consideration based on a more detailed discussion of nucleation kinetics involving the apportionment factor ψ, it is possible to clarify aspects of the model and to derive information concerning the molecular configuration associated with the activated state during stem attachment.

Relationship between σ' and initial length of cilia: thickness and other properties of the transient amorphous surface layer

The first objective is to obtain some idea of the thickness and nature of the transient ciliated surface layer in the vicinity of the nucleus in extended-chain crystallization before any significant annealing takes place. To do this we shall establish a relationship between σ' and the length of the protruding cilia. It is assumed that the nucleation and substrate completion processes are such that they initially leave a transient random distribution of cilium lengths limited to a maximum length of $l_{cil(max)}$ on each σ' surface emanating from a crystalline core of thickness l_c with stem length l_s (*Figure 2b*). This set of cilia of mean thickness l_a is assumed to result from the fact that the initial attachments of a molecule on the surface are not generally at the correct position to lead to well-matched end groups. This model is akin to the trapped molecule concept of Ungar and Keller[1], who suggested in pictorial terms that non-integral once-folding was caused in part by molecules nucleating initially on 'wrong' places on the substrate so that after deposition of the stem, one end of the molecule protruded over the edge of the crystal face. Below we treat the rather analogous situation for extended-chain surface nuclei (*Figure 2b*).

It is known from the statistical mechanical calculations of Lauritzen and DiMarzio[25] that the free energy change associated with the attachment at one end of a single cilium of contour length l_{cil} to a surface[7] is $\lambda kT \ln(l_{cil}/x_0)$. Here x_0 is the statistical segment length such that l_{cil}/x_0 is the number of statistical chain units in the cilium, and λ is a numerical factor dependent on the angle of sweep of the cilium (see below). For a set of cilia of random lengths ranging up to a maximum length $l_{cil(max)}$, which corresponds to the model in *Figure 2b*, the average free energy change per stem is readily shown for $l_{cil}/x_0 \geqslant \sim 3$ to be[26]:

$$\Delta G_{cil} = 2\lambda kT[\ln(l_{cil(max)}/x_0) - 1] \qquad (8)$$

where it is understood that this applies to both faces of the crystal. (The problem solved here is that of the free energy change associated with a chain of length $l_{cil(max)}$, which attaches at one point to a surface at random positions along its contour length; the shorter cilium is assigned at random to one face of the crystal, and the longer to the other face, the crystal core intervening between the two.) Here $\lambda = \pi/2\phi$ where ϕ is the angle of sweep of each cilium. For preliminary calculations we take x_0 to have the nominal value $C_n l_u \cong 6.7 \times 1.27 \times 10^{-8}$ cm $\cong 0.85$ nm, where C_n is the characteristic ratio. (It is taken as given that there exists a statistical segment length x_0 that determines thermodynamic properties of chain systems. The above proposition that x_0 is related to $C_n l_u$ is equivalent to the assumption that the statistical segment length that determines thermodynamic properties is of the same order as that which determines the spatial characteristics of the chain as described by C_n.) The corresponding transient surface free energy associated with the cilia on one end of the nucleus is therefore:

$$\sigma' = \lambda(kT/a_0 b_0)[\ln(l_{cil(max)}/x_0) - 1] \qquad (9)$$

This states in specific terms that σ' is the result of kinetically-induced ciliation on the end surface, and provides a more precise basis for the term 'rough' or 'disordered' surface in connection with the extended-chain problem.

Equation (9) is now applied to C-246. The calculations are made at $T_x = 122.3$°C, where real-time SAXS experiments show only extended-chain crystallization[1]. We use $\sigma' \cong 23$ erg cm^{-2} as found earlier for regime II and set $\lambda \cong 1/2$ as for $\phi = \pi$. Then it is found that $l_{cil(max)}$ corresponds to a cilium with a contour length of ~ 5 nm (*Table 2*). The average cilium contour length $\bar{l}_{cil}$ on each face is therefore ~ 2.5 nm giving the crystal an amorphous or disordered mass fraction in this transient state of:

$$\Phi_a = \frac{2\bar{l}_{cil}}{l_0} = \frac{2 \times 2.5 \text{ nm}}{31.52 \text{ nm}} \cong 0.16 \qquad (10)$$

Thus the transient originally-formed portion of the crystal of extended-chain C-246 is predicted to possess an amorphous layer of cilia of varying lengths of kinetic origin on each face, the sum of the two comprising $\sim 16\%$ of the mass. There is of course some latitude in this figure because of the uncertainty in σ' itself, as well as the uncertainties in λ and the precise value of x_0. However, we adhere to the general conclusion that at the very early stages of formation there is in fact a sizeable and unstable ciliated layer on the extended-chain crystal that is substantially thicker than the equilibrium value.

With the calculation cited above one can estimate a number of properties of the initially-formed extended-chain crystal. The stem length l_s in the crystal core is $l_0 - 2\bar{l}_{cil}$ or ~ 26.5 nm. Since the stems in the crystal are tilted at $\theta \cong 35°$ from the normal (corresponding to the {2 0 1} basal plane)[1] the initial crystal core thickness l_c comes to $l_s \cos\theta$ or ~ 21.7 nm. Then, as outlined in *Table 2*, it is found that each amorphous layer has a thickness l_a of ~ 2.9 nm when the density ratio cited in the table is taken into account. The total calculated thickness of the transient ciliated crystal of extended-chain C-246 is $l_c + 2l_a$ or 27.5 nm (*Table 2*).

The aforementioned real-time SAXS measurements at 122.3°C revealed that after ~ 15–20 min the Bragg reflections yielded a total crystal thickness for the extended-chain crystals of 25.7 nm, which is ~ 1.8 nm thinner than the estimate for the initially-formed transient crystal given above. At early times in the SAXS measurements, the first-order reflection[1] appears to us to imply a thickness greater than 25.7 nm, suggesting that some annealing had already occurred during the 15–20 min interval and that the younger extended-chain crystals may well have been slightly thicker, in qualitative accord with the above prediction. Careful consideration of the original SAXS data may verify this conjecture.

The initial kinetically-formed ciliated surface layer may

Table 2 Results for C-246

Quantity	Value	Origin
Folded species		
$\sigma_{e(\infty)}$ = fold surface free energy for fully folded ($f \to \infty$) surface	80 erg cm^{-2}[a]	Match of ΔT_1^* with equation (3) with $f = 1$
$\bar{\sigma}_{e(1)}$ = fold surface free energy for once-folded ($f = 1$) surface	40 erg cm^{-2}[a]	Equation (4)
Extended-chain species (initially-formed transient state)		
σ' = end surface free energy of initially-formed ciliated layer	23 erg cm^{-2} (regime II)	Match of T_{max}, *Figure 1c*
	29 erg cm^{-2} (regime I)	Match of T_{max}, *Figure 1b*
$l_{cil(max)}$ = mean maximum length of cilia in initial amorphous layer (one face)	5 nm	Equation (9) with $\sigma' = 23$ erg cm^{-2}, $x_0 = 0.85$ nm, $\lambda = 1/2$
$\bar{l}_{cil}$ = mean contour length of cilia in initial transient structure (one face)	2.5 nm	Calculated as $l_{cil(max)}/2$
Φ_a = mass fraction of initial crystal consisting of cilia of kinetic origin	0.16	Equation (10)
l_s = stem length (tilted $\sim 35°$) in core of initially-formed crystal	26.5 nm	Calculated as $l_0 - 2\bar{l}_{cil}$
l_c = crystal core thickness of initially-formed crystal	21.7 nm	Calculated as $l_c = l_s \cos 35°$
l_a = thickness of each transient ciliated surface layer	2.9 nm	Calculated as $l_0 \times \Phi_a(\rho_c/\rho_a)/2$
$l_{total(initial)}$ = total thickness of transient ciliated crystal before any annealing	27.5 nm	Calculated as $l_c + 2l_a$

[a]Nominal values based on $T_m = 128.6°C$ (see text)

exhibit some features associated with packing problems. It is now well understood that it is impossible to have normal random coils consisting of long flexible *n*-hydrocarbon chains emanating from every surface site unless the points of departure from the crystal are separated by tilting the chains about $\theta \cong 70.5°$, i.e. $\cos^{-1}\theta \cong 1/3$. With $\theta = 0$ as for vertical stems, a serious density paradox obtains in such a system[27–30]. In the present situation, this problem is considerably mitigated by the mixture of short and long cilia on the surface and the angle of tilt of $\theta \cong 35°$. Nevertheless, our preliminary estimate is that it would require an angle of tilt somewhat larger than this to completely avoid any remnant of the density paradox. Thus, with the actual angle of tilt being $\sim 35°$, one anticipates that some crowding may occur, causing orientation in the ciliated surface layer; at least part of the layer may exhibit order of a liquid crystalline character near the melting point. (At sufficiently low temperatures, the ciliated surface phase is likely crystal- or glass-like). This crowding, if present, would contribute additionally to σ' as the 'polymer in a cone' calculation shows[31]. Also any crowding present would cause surface stresses and contribute to forcing the system to reduce the ciliation on the surface during annealing. Surface stresses can also lead to the crystals exhibiting curved edges[7].

Whatever the details of the nature of the initial ciliated amorphous phase, it is evident that in addition to giving rise to σ' in growth rate experiments, this phase will contribute significantly to the thermodynamic properties of the system as long as it persists and is at a temperature where it is not crystal- or glass-like. For example, the transient ciliated surface phase must be expected to be active in contributing to the heat capacity well below T_m, leading to so-called pre-melting effects. Such effects have been found in C-192 and attributed to conformational disorder of the chain ends[10]. The ciliated amorphous phase is surprisingly persistent, taking considerable time to be even partly erased (see below). It is our expectation that the pre-melting effects would be lessened if d.s.c. runs were obtained on extended-chain specimens that had been previously crystallized or annealed for a very prolonged period near T_m. A related aspect of the presence of the ciliated amorphous layer predicted earlier to exist in a fresh specimen is that it will reduce the latent heat of fusion at T_m below its true equilibrium value. If one provisionally accepts the estimate of $\Phi_a \cong 0.16$ in equation (10) for C-246, the latent heat of fusion for a fresh specimen of this material could be as much as 16% low. A deficiency in the latent heat of fusion as high as 15% was found by d.s.c. measurements for C-192, pre-melting effects making up part of the difference[10]. The T' *versus* T_x plot for C-192, to be discussed shortly, speaks compellingly to the point that very long periods of time are required to establish equilibrium behaviour in such systems. Accordingly, we are inclined to attribute highly conspicuous pre-melting effects and large deficiencies in the latent heat of fusion in extended-chain specimens crystallized under conventional conditions largely to the remaining transient amorphous layer, as opposed to assuming that these effects represent true equilibrium phenomena to be treated by a theory based on the same assumption. This does not preclude the existence of some residual pre-melting effects resulting from the onset of molecular motions associated with the equilibrium degree of ciliation.

Annealing of extended-chain crystals

The treatment has it that in an 'as-born' extended-chain crystal, the kinetically-induced ciliated surface layer is unstable: such a crystal has a relatively large σ' and by equation (1) will have a melting point T' that is noticeably below T_m. Such a crystal will strive towards equilibrium by reducing the thickness of the ciliated surface layers, causing σ' to fall as described by equation (9). (Simultaneously the core thickness l_c will increase.) During this process T' will increase according to equation (1) because of the diminution of σ'. A small net decrease in total thickness may take place concurrently, owing to the shrinkage of the less dense surface phase: this would parallel the thinning of the initial once-folded species on annealing observed in real-time SAXS experiments by

Ungar and Keller and depicted schematically in *Figures 3a* and *b*. The extended-chain system will strive toward one where there is an equilibrium degree of roughness consisting of some quite short cilia perhaps with some paired chain ends. The melting point of the fully annealed extended-chain crystal with an equilibrium degree of ciliation is the true T_m.

We must now ask if there is any direct evidence that annealing of extended-chain crystals leads to an increase of melting point with increased time of isothermal storage. This would imply a diminution with time of σ', and concomitant thinning of the transient surface amorphous zone. The process we have in mind is that depicted in *Figure 5a*. Definite evidence along this line has been found by Stack *et al.* for pure C-192 in the form of a T' *versus* T_x (Hoffman–Weeks) plot which they give in Figure 6 of ref. 10. The general situation is shown schematically in *Figure 5b*. The data points in the original work in the linear region of the T' *versus* T_x plot ($T_x \cong 119$–125°C) refer exclusively to extended-chain crystallization, the once-folding effect proposed by us earlier appearing only below 116–117°C. At a low crystallization temperature where the crystallization was rapid, as shown by the $\tau_{0.05}^{-1}$ data in Figure 10 of ref. 10, and the residence time therefore short, the melting point was about 1.3°C below the limiting upper value. We interpret this surprising and heretofore unexplained result as showing that σ' was fairly large because the transient ciliation effect proposed here had not had time to closely approach the equilibrium state. Through equation (1) the value of σ' is estimated to be ~ 11 erg cm^{-2}. At a higher crystallization temperature, significant annealing had taken place because of the considerably longer residence time resulting from the much slower crystallization process as evidenced by the corresponding $\tau_{0.05}^{-1}$ data, and the melting point was notably higher (*Figure 5*). The extrapolation of the data to the line $T' = T_x$ for C-192 yields $T_m = 127.5$°C, which may be taken as a close estimate of the true equilibrium melting point as indicated by Stack *et al.*[10]. It can be shown that this extrapolation is essentially to infinite residence time. (The derivation of the T' *versus* T_x plot in this case differs from that[4] for chain-folded systems.) At the intersection of the extrapolated data points with the line $T' = T_x$, the amorphous ciliated surface layer should have its equilibrium thickness. The thickness of this layer is not currently known, but it is certainly small (see below).

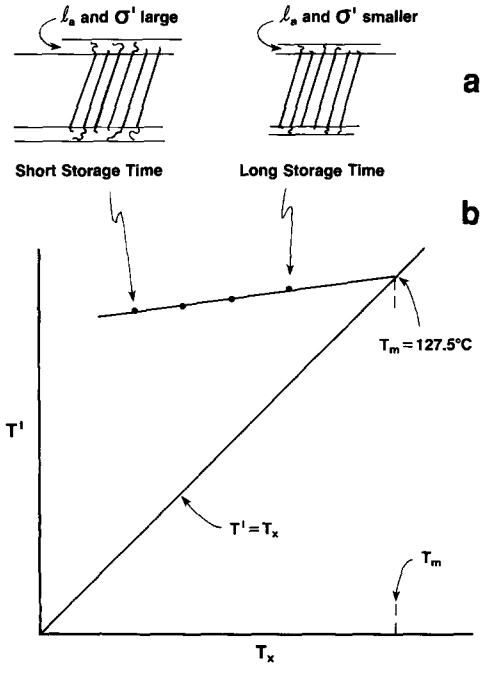

Figure 5 Annealing of extended-chain C-192. (a) Schematic of proposed changes in structure as function of storage time. (b) Schematic diagram of T' *versus* T_x plot of Stack *et al.*[10] showing nature of their extrapolation to obtain close estimate of true equilibrium melting point T_m

Apart from supporting the mechanism proposed here for annealing of extended-chain crystals, the results mentioned above have some interesting ramifications. First, the time scale for the attainment of equilibrium is surprisingly long, as the T' *versus* T_x plot combined with the $\tau_{0.05}^{-1}$ data for C-192 shows. This implies that the equilibrium melting points of some of the longer pure *n*-paraffins quoted in the literature, which were obtained by conventional procedures, may be somewhat low. It is for this reason that we supposed earlier that the true T_m of C-246 may be somewhat higher than 128.6°C. It follows also that the true equilibrium thickness of the rough surface layer and the true latent heat of fusion and related properties may only be attainable by very prolonged experiments or by extrapolation techniques; in experiments of ordinary duration only a transient value of these quantities is apt to be observed. The next point is that the commonly accepted analysis for estimating the equilibrium melting point, namely that of Flory and Vrij[32], assumes paired chain ends, i.e. no equilibrium roughness. We observe in this connection that Broadhurst's version[33] of the Flory–Vrij treatment, which has a T_m for $n \to \infty$ of 144.7°C, leads to a T_m of 128.02°C for C-192. This is only ~ 0.5°C above the result obtained by Stack *et al.*[10] by the T' *versus* T_x extrapolation method. One possible implication of this rather close agreement is that the true equilibrium thickness $l_{a(eq)}$ of the ciliated amorphous surface layer is quite small. Finally, it is evident that it would be of value to apply the T' *versus* T_x technique to C-198, C-246, and other pure *n*-paraffins to obtain close estimates of T_m. It is only with such T_m data that a more precise analysis of the maximum in the extended-chain growth rate of C-246 and related *n*-paraffins can be effected. The same is true for obtaining the best $\sigma_{e(\infty)}$ to use in calculating ΔT_f^* with equation (3). We judge the T' *versus* T_x plot to be the best method currently available to estimate T_m values appropriate to the equilibrium state for the *n*-paraffins.

A theoretical estimate of the general magnitude of the equilibrium surface roughness (equilibrium ciliation) may be obtained from the treatment of Lauritzen and Passaglia[14] as recalculated[34] for a σ of 13 erg cm^{-2}. Fortunately, this surface roughness calculation involves a system with stems comparable in length to those of interest here and depends only on σ and not σ_e; the σ energy associated with a protruding stem is the principal variable. Hence the calculation has more than a distant relevance to an extended-chain system. As Figure 14 of ref. 34 shows, the root-mean-square deviation is ~ 6 Å at $\Delta T \to 0$, i.e. at true equilibrium. This may be taken as an approximate estimate of $l_{a(eq)}$. The calculation applies to an isolated lamella. (It is not exactly clear what the result would be for a stack of lamellae, though it would be reasonable to suppose that if different it would be

smaller.) Whatever the approximations in this calculation, it is evident that the equilibrium degree of surface roughness is much less than that of the transient ciliated layer originally present in an embryonic extended-chain crystal.

If $l_{a(eq)}$ is indeed as small as estimated above, the prospect of an equation of the Flory–Vrij type fitting the equilibrium T_m values for the *n*-paraffins would appear to be good. The key is of course to use T_m values obtained by the T' *versus* T_x method as input data. While the chain ends would not be paired in the Flory–Vrij sense with such an $l_{a(eq)}$, the correction for this effect is likely to be small. By obtaining T_m values by the T' *versus* T_x method for the longer *n*-paraffins it may well be possible to secure a more reliable and even widely agreed upon estimate of T_m for $n \to \infty$ for the $(-CH_2-)_n$ system.

Molecular conformation during nucleus formation in extended-chain systems: interpretation of ψ and origin of σ

Further consideration is now given to what the apportionment factor ψ reveals about the nature of the activated state during the stem attachment process. This will include a more complete discussion of the origin of σ, and comments concerning how ψ relates to nucleation theory generally.

The maximum in the growth rate of C-246 between T_m and T_1^* can only be reproduced for low values of ψ. A low value of ψ means that only the small fraction $\psi a_0 b_0 l_0(\Delta G)$ of the free energy of fusion per molecule (work of stem attraction to substrate) has been realized when the activated state is attained (see equation (A-2) of the Appendix). The implication is that in the activated state, the molecule has but few strictly crystallographic attachments as shown schematically in *Figure 2b*. This leads to an activated state wherein the molecule is highly restricted on the surface at which time σ is established. This bears the clear implication that in chain systems σ is largely of entropic origin, i.e. it is mainly the result of the fact that the molecule is closely confined to the surface (see below). (The corresponding rigid rod model, and the apparently attractive regular 'zippering down' model, both give $\psi \cong 1$; neither permits the maximum in the extended-chain growth rate to be accounted for.) Once this activated state with its few crystallographic attachments is attained, a full stem (except for the ciliated ends) rapidly forms on the core at a rate A_0' (*Figure 2b*). This is important, since it describes in a physically plausible manner how a crystallographically coherent core is achieved, an obvious requirement of any theory of crystallization. This rapid process is attended by the free energy of fusion $(1-\psi)a_0 b_0 l_0(\Delta G)$. As seen from equation (A-3) of the Appendix, the backward reaction for the removal of the first stem with detailed balance considered, naturally requires that this same large free energy of fusion of $(1-\psi)a_0 b_0 l_0(\Delta G)$ be supplied to remove it from the substrate.

A similar set of circumstances involving A' in *Figure 2b* applies to the substrate completion process, $v \geqslant 2$. (Recall that for more complete rigour, l_0 in the above expressions should be replaced by $l_0 - 2\bar{l}_{cil}$; this does not alter the basic argument.) Inclusion of the backward (stem removal) reactions under the condition of detailed balance is utterly essential in the present application, for without them neither the maximum in the growth rate in the extended-chain domain of C-246 nor the $G \propto \Delta T$ behaviour of C-94 near the melting point could have been understood.

The concept noted above that σ is generated by the localization of a chain by a few crystallographic or other specific attachments to a substrate can be supported in a semiempirical manner. By equating the work of (a) converting a chain in a random coil configuration in the melt as scaled to account for its segmental character to a configuration where the chain is highly confined near the crystal substrate but crystallographically attached to it at only a few sites (i.e. has a low entropy with respect to the melt but virtually no actual heat of fusion) to (b) the work of forming the two lateral surfaces $2b_0\sigma l_0$, one can deduce the approximate relationship for the entropic contribution to lateral surface free energy:

$$\sigma_{theor} \simeq \frac{T}{2}\left(\frac{\Delta h_f}{T_m}\right) a_0 \left(\frac{l_u}{x_0}\right) \tag{11}$$

where l_u is the length of a chain unit and x_0 the statistical segment length appropriate to thermodynamic properties. For a $(-CH_2-)_n$ system where n is large, this gives $\sigma_{theor} \cong 10$ erg cm^{-2} for $x_0 = 8$ Å and $l_u = 1.273$ Å. Recalling that experimental σ values for this system fall in the range 13.8 ± 2.1 erg cm^{-2}, the concept that σ is largely of entropic origin is evidently well founded. Reversing the procedure and calculating x_0 with $\sigma = 13.8 \pm 2.1$ erg cm^{-2} yields $x_0 = 5.9 \pm 0.8$ Å, a nominally reasonable value for the statistical segment length relevant to thermodynamic effects. With σ values for other vinyl polymers, equation (11) gives values of x_0 in the range of ~5–10 Å, which bear a close relation to published C_n data. This provides further support for the mostly entropic origin of σ in chain systems. A full report concerning the application of equation (11) will be made elsewhere[35]. In their studies of homogeneous nucleation in *n*-alkanes C-5 to C-32, Turnbull and Spaepen[36] demonstrated that the segmental character of the longer chains played a role in causing the scaled interfacial tension to settle down to a constant value near C-15; there is a clear implication in this work that σ is of mostly entropic origin.

It remains to place the apportionment factor ψ in a more general perspective. The wellspring of virtually all modern nucleation treatments, i.e. that of Turnbull and Fisher[37], implicitly assumes the sensible value $\psi = 1/2$ for the case of small non-chain atoms or molecules. These authors considered both forward and backward reactions, and when this is done there is no option other than to decide on the relative weighting of these reactions for the system at hand. Thus, the introduction of ψ in nucleation theory is of long standing. In the present work the data on C-246 demanded a low value of ψ to obtain the maximum in the growth rate of the extended-chain species, and this low ψ in turn showed that the basic nature of the activated complex corresponded to the partial stem attachment model illustrated schematically in *Figure 2b*. On reflection, one sees this model as fully reasonable in such a system: it is too much to expect that in the surface nucleation act the chain would nucleate at the outset as a rigid rod, or fit one end neatly on the edge of the substrate and then 'zipper down' in perfect register with no overhang on the other end. In addition, the low ψ effect leads to the important conclusion that σ is in the general sense associated with the localization of the long molecules on the substrate as promulgated

by relatively few strictly crystallographic or other attachments, as was originally suggested for chain-folded systems[4]. The factor ψ is a physically real quantity that illuminates molecular aspects of the nucleation process in chain systems that would otherwise escape explanation.

SUMMARY AND CONCLUSIONS

Flux-based nucleation theory can deal with major aspects of extended-chain crystallization and the extended-chain to once-folded transition in specific systems in a straightforward manner and in some detail. The onset of once-folding for molecules of fixed length l_0 occurs when the kinetically-determined surface nucleus length l_g^* falls close to $l_0/2$. The value of l_g^* is a variable, and depends on the undercooling and the effective fold surface free energy as obtained with a mean field approximation to account for both folds and chain ends. The treatment holds quantitatively for poly(ethylene oxide) fractions, and appears to be valid for C-192, C-198 and C-246. In contrast, the molecular length active in the extended-chain surface nucleus is a constant close to l_0, which turns out to be the main cause of the maximum that appears in the growth rate below the melting point in C-246. The presence of a minimum in the growth rate below the maximum follows directly.

The activated complex associated with the extended-chain nucleus has a partial stem attachment feature, which is involved in predicting the maximum. This same feature brings out the entropic origin of the lateral surface free energy, which opposes the addition of the first stem. The initially-formed extended-chain crystal has a rough (i.e. ciliated) end surface arising from mismatch of the chain ends during surface nucleation. The resulting amorphous surface layer is treated as consisting of cilia of varying lengths. The thickness of the amorphous layer in the embryonic extended-chain crystal, as estimated from an end surface free energy σ' from growth rate data for C-246 combined with a statistical mechanical treatment, is substantially larger than the equilibrium value. The initially-formed amorphous layer is unstable, and slowly becomes thinner on annealing. The thinning of the ciliated amorphous surface layer is accompanied by changes in physical properties, e.g. an increase of melting point with increased storage time as is observed in extended-chain C-192.

ACKNOWLEDGEMENT

Special thanks are due to Drs Robert L. Miller and Marc L. Mansfield of the Michigan Molecular Institute for invaluable comments and advice.

REFERENCES

1 Ungar, G. and Keller, A. *Polymer* 1987, **28**, 1899
2 Hoffman, J. D. *Macromolecules* 1985, **18**, 772
3 Hoffman, J. D. *Macromolecules* 1986, **19**, 1124
4 Hoffman, J. D., Davis, G. T. and Lauritzen, J. I. Jr in 'Treatise on Solid State Chemistry' (Ed. N. B. Hannay), Plenum, New York, 1976, Vol. 3, Ch. 7, pp. 497–614
5 Lauritzen, J. I. Jr and Hoffman, J. D. *J. Appl. Phys.* 1973, **44**, 4340
6 Hoffman, J. D. and Miller, R. L. *Macromolecules* 1989, **22**, 3038
7 Hoffman, J. D. and Miller, R. L. *Macromolecules* 1988, **21**, 3038; Miller R. L. and Hoffman, J. D. *Polymer* 1991, **32**, 963
8 Lauritzen, J. I. Jr and Hoffman, J. D. *J. Res. Natl. Bur. Stand., Sect. A* 1960, **64**, 73
9 Fletcher, D. P. and Klein, J. *Polym. Commun.* 1985, **26**, 2
10 Stack, G. M., Mandelkern, L., Kröhnke, C. and Wegner, G. *Macromolecules* 1989, **22**, 4351
11 Paynter, D. I., Simmonds, D. J. and Whiting, M. C. *J. Chem. Soc. Chem. Commun.* 1982, 1165
12 Bidd, I. and Whiting, M. C. *J. Chem. Soc. Chem. Commun.* 1985, 543
13 Frank, F. C. and Tosi, M. *Proc. R. Soc. London, Ser. A* 1961, **263**, 323
14 Lauritzen, J. I. Jr and Passaglia, E. *J. Res. Natl. Bur. Stand., Sect. A* 1967, **71**, 261
15 Hoffman, J. D. *Polym. Commun.* 1986, **27**, 39
16 Kovacs, A. J., Gonthier, A. and Straupe, C. *J. Polym. Sci., Polym. Symp.* 1975, (50), 283
17 Kovacs, A. J., Straupe, C. and Gonthier, A. *J. Polym. Sci., Polym. Symp.* 1977, (59), 31
18 Kovacs, A. J. and Straupe, C. *J. Cryst. Growth* 1980, **48**, 210
19 Kovacs, A. J. and Straupe, C. *Faraday Discuss. Chem. Soc.* 1979, (68), 225
20 Point, J. J. and Kovacs, A. J. *Macromolecules* 1980, **13**, 399
21 Keller, A. and Udagawa, Y. *J. Polym. Sci., Part A-2* 1972, **10**, 221
22 D'Ilario, L., Keller, A. and Martuscelli, E. *J. Polym. Sci., Part A-2* 1972, **10**, 239
23 Ungar, G., Stejny, J., Keller, A., Bidd, I. and Whiting, M. C. *Science* 1985, **229**, 386
24 Ungar, G., Organ, S. J. and Keller, A. *J. Polym. Sci., Part C: Polym. Lett.* 1988, **26**, 259
25 Lauritzen, J. I. Jr and DiMarzio, E. A. *J. Res. Natl. Bur. Stand. (US)* 1978, **83**, 381
26 Mansfield, M. L. Michigan Molecular Institute, private communication
27 Guttman, C. M. and DiMarzio, E. A. *Macromolecules* 1982, **15**, 525
28 Guttman, C. M., DiMarzio, E. A. and Hoffman, J. D. *Polymer* 1981, **22**, 1466
29 Mansfield, M. L. *Macromolecules* 1988, **21**, 126
30 Frank, F. C. *Faraday Discuss. Chem. Soc.* 1979, (68), 7
31 Guttman, C. M., DiMarzio, E. A. and Hoffman, J. D. *J. Res. Natl. Bur. Stand. (US)* 1980, **85**, 273
32 Flory, P. J. and Vrij, A. *J. Am. Chem. Soc.* 1963, **85**, 3548
33 Broadhurst, M. G. *J. Res. Nat. Bur. Stand., Sect. A* 1966, **70**, 481
34 Hoffman, J. D., Lauritzen, J. I. Jr, Passaglia, E., Ross, G. S., Frolen, L. J. and Weeks, J. J. *Kolloid Z. Z. Polym.* 1969, **231**, 564
35 Hoffman, J. D. manuscript in preparation
36 Turnbull, D. and Spaepen, F. *J. Polym. Sci., Polym. Symp.* 1978, (63), 237
37 Turnbull, D. and Fisher, J. C. *J. Chem. Phys.* 1949, **17**, 71

APPENDIX

Derivation of growth rate expressions for extended chains and relationship to rate expression for chain folding

The flux-based treatment follows the pattern employed elsewhere to find growth rates controlled by surface nucleation events[4–7]. The standard state is the liquid at T_m. From a consideration of surface thermodynamics associated with the model in *Figure 2a*, the free energy change on adding the vth stem on the substrate is:

$$\Delta\phi_v = 2b_0\sigma l_0 + 2a_0b_0\sigma' - a_0b_0l_0(\Delta G) - a_0b_0(v-1)[l_0(\Delta G) - 2\sigma'] \quad \text{(A-1)}$$

The rate of addition of the first stem ($v = 1$) is controlled by:

$$A_0 = \beta \exp -\frac{2b_0\sigma l_0}{kT} \exp -\frac{2a_0b_0\sigma'}{kT} \exp \frac{\psi a_0b_0l_0(\Delta G)}{kT} \quad \text{(A-2)}$$

and the rate of the corresponding backward reaction for stem removal is:

$$B_1 = \beta \exp \frac{-(1-\psi)a_0b_0l_0(\Delta G)}{kT} \quad \text{(A-3)}$$

The rate for the forward reaction for each substrate stem addition ($v \geqslant 2$) is:

$$A = \beta \exp -\frac{2a_0b_0\sigma'}{kT} \exp \frac{\psi a_0b_0l_0(\Delta G)}{kT} \quad \text{(A-4)}$$

and each of the corresponding backward reactions is governed by:

$$B = \beta \exp -\frac{(1-\psi)a_0b_0l_0(\Delta G)}{kT} \quad \text{(A-5)}$$

In the above, the retardation parameter describing transport of segments in the melt to the crystal surface is in events per second.

$$\beta = \frac{\kappa}{n}\left(\frac{kT}{h}\right)\exp(-Q_D^*/RT) \quad \text{(A-6)}$$

where n is the number of chain units and κ is a number of the order of unity derivable from the friction coefficient[7]. The apportionment factor ψ, confined in principle to values between zero and unity, describes for A_0 and A the fraction of the free energy of fusion per stem that is attained just as the activated state is reached. Note especially that the ratios A_0/B_1 for $v = 1$ and A/B for $v \geqslant 2$ yield the equilibrium distributions according to equation (A-1), thus preserving detailed balance for any allowable value of ψ.

The total flux across the barrier system shown in *Figure 2a* is given by the exact relation[4]:

$$S_T = \frac{N_0A_0(A-B)}{A-B+B_1} = \frac{N_0A_0(A-B)}{A} \quad \text{(A-7)}$$

the second equality holding for $B = B_1$ as in equations (A-3) and (A-5). Here $N_0 = C_0n_s$ is the number of reacting species, C_0 is configurational path degeneracy, and n_s is the number of stems comprising the substrate of length $L = n_sa_0$. Then, with the nucleation rate i being defined as $S_T/L = S_T/a_0n_s$ as is customary, noting that the substrate completion rate is defined as $g \equiv a_0(A-B)$, and remembering the formal definitions of regime I ($G_I \equiv b_0iL$) and regime II ($G_{II} \equiv b_0(2ig)^{1/2}$), one obtains the growth rate expressions given in the text as equations (2a) and (2b) with the pre-exponential factors given below. For equation (2a):

$$G_{0(I)} = C_0n_s\left(\frac{\kappa}{n}\right)\left(\frac{b_0kT}{h}\right)\exp\frac{\psi a_0b_0l_0(\Delta G)}{kT} \quad \text{(A-8)}$$

and for equation (2b):

$$G_{0(II)} = (2C_0)^{1/2}\left(\frac{\kappa}{n}\right)\left(\frac{b_0kT}{h}\right)\exp\frac{\psi a_0b_0l_0(\Delta G)}{kT} \quad \text{(A-9)}$$

Note that for extended-chain growth the nucleus length l_0 is held constant (subject to the small correction to account for ciliation mentioned in the main text).

For chain-folded growth, the nucleus length is properly treated as a variable and the total flux is then calculated as[4–7]:

$$S_T = \frac{1}{l_u}\int_{2\sigma_e/(\Delta G)}^{\infty} \frac{N_0A_0(A-B)}{A}\mathrm{d}l \quad \text{(A-10)}$$

The lower limit represents the fold period of the thinnest possible, i.e. just stable, crystal. The rates A_0, B_1, A and B for the chain-folded case are given in various places[4–7] and lead straightaway to the growth rate for regime II:

$$G_{II(fold)} = G_0(\Delta T)\exp(-Q_D^*/RT)\exp -\frac{2b_0\sigma\sigma_eT_m}{(\Delta h_f)(\Delta T)kT} \quad \text{(A-11)}$$

from which equation (6a) is adapted. The variation of the nucleus length in the chain-folded case is also flux-determined according to[4–7]:

$$l_g^* = \frac{1}{l_u}\int_{2\sigma_e/(\Delta G)}^{\infty} lS(l)\,\mathrm{d}l \Big/ \frac{1}{l_u}\int_{2\sigma_e/(\Delta G)}^{\infty} S(l)\,\mathrm{d}l = \frac{2\sigma_e}{\Delta G} + \delta \quad \text{(A-12)}$$

where $S(l) = N_0A_0(A-B)/(A-B+B_1)$. This leads directly to equation (5) when $\bar{\sigma}_e$ is substituted for σ_e.

While the growth rates of both extended-chain and chain-folded structures are determined by the net rate of passage (total flux) over a barrier of the type shown in *Figure 2a*, the foregoing highlights the fundamental difference in the approach that must be employed to properly treat them. In both cases, a ψ well below unity is commonly required to deal with real chain systems, implying that the partial stem attachment model for the activated complex is the norm[4–7].